



OPEN

Identification and characterization of a novel heparinase PCHeplI from marine bacterium *Puteibacter caeruleilacunae*

Danrong Lu, Luping Wang, Zeting Ning, Zuhui Li, Meihua Li, Yan Jia & Qingdong Zhang

Heparin (HP) and heparan sulfate (HS) are multifunctional polysaccharides widely used in clinical therapy. Heparinases (Hepases) are enzymes that specifically catalyse HP and HS degradation, and they are valuable tools for studying the structure and function of these polysaccharides and for preparing low molecular weight heparins. In this study, by searching the NCBI database, a novel enzyme named PCHeplI was discovered in the genome of the marine bacterium *Puteibacter caeruleilacunae*. Heterologously expressed PCHeplI in *Escherichia coli* (BL21) has high expression levels and good solubility, active in sodium phosphate buffer (pH 7.0) at 20°C. PCHeplI exhibits an enzyme activity of 254 mU/mg towards HP and shows weak degradation capacity for HS. More importantly, PCHeplI prefers to catalyse the high-sulfated regions of HP and HS rather than the low-sulfated regions. Although PCHeplI functions primarily as an endolytic Hepase, it mainly generates disaccharide products during the degradation of HP substrates over time. Investigations reveal that PCHeplI exhibits a preference for catalysing the degradation of small substrates, especially HP tetrasaccharides. The catalytic sites of PCHeplI include the residues His¹⁹⁹, Tyr²⁵⁴, and His⁴⁰³, which play crucial roles in the catalytic process. The study and characterization of PCHeplI can potentially benefit research and applications involving HP/HS, making it a promising enzyme.

Glycosaminoglycans are a group of polyanionic and heterogeneous polysaccharides containing heparin (HP) and heparan sulfate (HS). HP and HS consist of repeating disaccharides, which consist of D-glucuronic acid/L-iduronic acid (GlcA/IdoA) and N-acetyl-D-glucosamine (GlcNAc)¹. These polysaccharides have a broad distribution, and they are present on the surfaces of cells, in the extracellular matrix (ECM), and even within the intracellular environment (found in mast cells)². Modification of the common precursor of HP and HS involves multiple enzymes, such as sulfotransferases that can selectively add sulfate groups to GlcA/IdoA (2S) or GlcNAc (3S, 6S, NS) residues and epimerases that can convert some GlcA to IdoA, resulting in highly complex HP and HS^{3,4}. As a result, the HP polysaccharides are mainly composed of the trisulfated disaccharide unit -4 IdoA2S1-4 GlcNS6S, and the degree of sulfation was approximately 2.7. HS mainly consists of lower-sulfated disaccharide units, and the degree of sulfation is lower than that of HP⁵. HP and HS, which are composed of numerous variations of disaccharides, are the most intricate polymers that exist in nature⁴.

The intricacy of the HP and HS structure allows them to participate in numerous physiological and pathological mechanisms, for example, HP is known to function as an anticoagulant⁶. Since its identification in the 1920s, HP and low molecular weight heparins (LMWHs) have been extensively utilized as a prominent category of anticoagulants in clinical therapy¹. In addition, HP and its related compounds have been found to exhibit various other biological functions, including roles in cellular adhesion⁷, inflammation⁸, cellular migration⁹, differentiation¹⁰, and even pathogenic infection¹¹. These functions are mediated through interactions with different signalling proteins^{7,12,13}. Given the significant biological functions of HP and its related compounds, there has been considerable interest in both structural and functional research on these compounds, as well as their clinical applications.

Heparinases (Hepases) are a group of enzymes in the polysaccharide lyase families derived from bacteria. They utilize a β -elimination reaction to breakdown HP and HS and produce oligosaccharide products with unsaturated double bonds at the nonreducing end¹². Hepases can be classified into three types: Hepase I (EC4.2.2.7), Hepase II (EC 4.2.2.-), and Hepase III (EC 4.2.2.8), each with distinct substrate preferences: Hepase I prefers to

School of Life Science and Technology, Weifang Medical University, 7166 Baotong West Street, Weifang 261053, China. email: zhangqingdong@wfmuc.edu.cn

catalyse high-sulfated HP, Hepase III prefers to degrade low-sulfated HS, and Hepase II can effectively digest both polysaccharides (Fig. 1)¹⁴. The widely used Hepases are Hepase I, Hepase II, and Hepase III from *Pedobacter heparinus* DSM 2366 (formerly known as *Flavobacterium heparinum*)^{15–17}. These Hepases are typically employed to examine the precise composition of HP and HS and for the preparation of LMWHs. For example, the widely used drug tinzaparin is prepared via the partial degradation of HP polysaccharides by Hepase I¹⁸.

The commercial hepases currently available are mainly extracted from fermentation broths of *P. heparinus* DSM 2366, but they have a relatively high selling price. Therefore, researchers have turned to heterologous hepases from *P. heparinus* DSM 2366 and to the identification of novel hepases from other bacteria. New variants of Hepase I, Hepase II and Hepase III have been discovered in various bacterial strains, such as *Bacteroides stercoris* HJ-15^{19–21}, *Bacteroides thetaiotaomicron* (BT4657)^{14,22}, *Bacillus circulans* HpT298²³, *Prevotella heparinolytica*²⁴, *Bacteroides eggerthii* VPI T5-42B-1²⁵, *Bacteroides cellulosilyticus*²⁶, *Raoultella* sp. NX-TZ-3-15^{27,28}, and *Streptomyces variabilis* MTCC 12266²⁹. Additionally, new families of Hepases, known as exolytic Hepases, have recently been identified³⁰. However, while Hepases derived from terrestrial bacteria have been extensively researched and reported, the novel Hepases from specialized marine environments that may possess novel characteristics have not yet been documented³¹.

This research presents the identification and report of the novel Hepase PCHeP2, an enzyme from a marine bacterium. This study provides a detailed analysis of the enzyme's properties, including its enzymatic characteristics, substrate catalytic modes, substrate preferences, and structure of the catalytic sites. The marine hepase PCHeP2 exhibits efficient degradation capabilities, suitable enzymatic properties, and a preference for catalysing small-sized oligosaccharide substrates. The results indicate that PCHeP2 may serve as a beneficial tool to perform structural investigations on HP and HS.

Material and methods

Materials

The PCHeP2 gene from *Puteibacter caeruleilacunae* (GenBank code: TKG96895.1) was selected from the National Center for Biotechnology Information (NCBI) GenBank database. Vazyme Biotech, Inc. provided the *Escherichia coli* competent BL21 cells (DE3) (Nanjing, China). Hyaluronate (HA) (BR degree), chondroitin sulfate (CS) (BR degree), dermatan sulfate (DS) (BR degree), sodium alginate (BR degree), 2-aminobenzamide (2-AB), and sodium cyanoborohydride (NaBH₃CN) were obtained from Sigma–Aldrich Inc. Hepase I, Hepase II and Hepase III were provided by the Fuchuan Li Laboratory. HP (BR degree) from porcine intestinal mucosa was purchased from Hefei BOMEI Biotechnology Co., Ltd. (Anhui, China). HS was extracted from porcine intestinal mucosa³². The HP oligosaccharides were prepared by partially digesting HP polysaccharides using Hepase I followed by gel filtration chromatography on a Superdex 30 Increase 10/300 GL column, and the detailed methods are provided in the Supplementary materials. China National Medicines Corporation Ltd. (Beijing, China) supplied all the chemicals and reagents mentioned in this paper.

Sequence analysis of the PCHeP2 gene and protein

The DNA and protein sequences of PCHeP2 were obtained from the NCBI database. The G + C% content of pchep2 was computed using Bio-Edit version 7.0.9. The theoretical molecular weight (Mw) and isoelectric point (pI) of the PCHeP2 protein were determined using the ExPASy server of the Swiss Institute of Bioinformatics and the peptide estimation tool. To determine the type of PCHeP2 and its corresponding secretion signal peptide, the SignalP 5.0 server was used for prediction. Phylogenetic analysis and amino acid alignment, including that of newly identified hepases, were performed using MEGA version 7.0. To gain insight into the function and sequence similarity of the enzymes, functional annotation and sequence similarity analysis were carried out by searching for amino acid sequences online using the NCBI's online BLAST algorithm. Identification of the protein modules and functional domains of PCHeP2 was achieved by utilizing SMART, the Pfam database, and the Carbohydrate-Active Enzyme database.

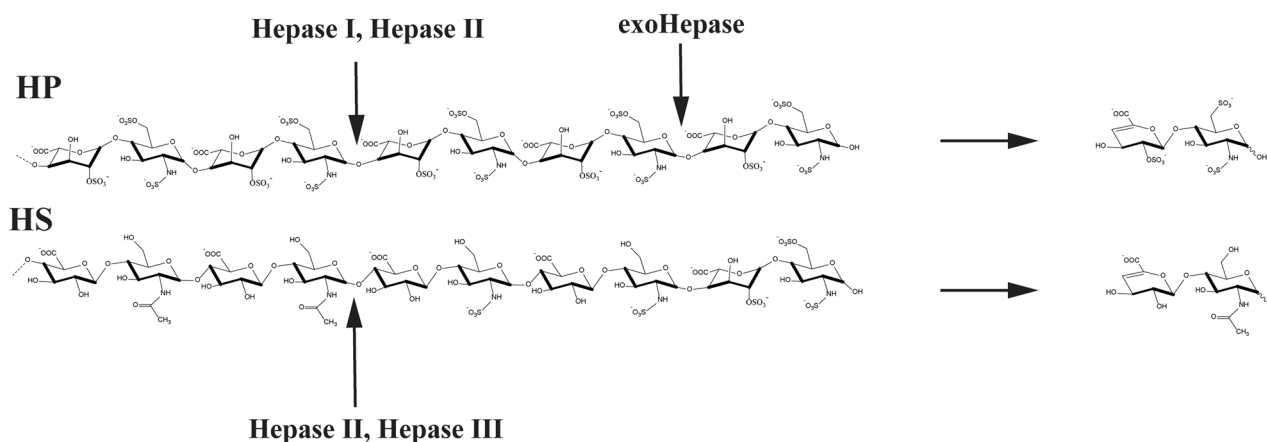


Figure 1. Substrate preference of Hepase I, Hepase II and Hepase III.

Heterologous expression and purification of PCHeplII

The *pcheplII* gene was artificially synthesized by the company GENEWIZ, Inc., located in Suzhou, China. Then, it was combined with the vector pET-30a (+) to generate the recombinant plasmid pET30a-*pcheplII*, which carries a C-terminal (His)₆-tag. The recombinant plasmid was transformed into competent *E. coli* BL21 (DE3) cells by heat shock at 42°C for 1 min. Positive colonies of *E. coli* BL21-pET30a-*pcheplII* were verified by the gene sequencing process in Sangon Biotech (Shanghai, China) and cultivated in fresh LB broth supplemented with kanamycin at a final concentration of 0.05 mg/mL. Cultivation was carried out at 37°C and 200 rpm until the cell density reached 0.6–0.8 (OD₆₀₀). Once the desired cell density was achieved, the mixture was cooled to 16°C, and agitation at 220 rpm was employed to induce the synthesis of the target protein PCHeplII. This was achieved by adding 0.05 mM IPTG and allowing protein expression to proceed for 18–24 h.

For the subsequent steps, the fermentation broth was resuspended in prechilled buffer A, which consisted of 50 mM Tris-HCl and 150 mM NaCl and had a pH of 8.0. Centrifugation was then carried out at 8000 × g for 10 min to collect the cells. Next, the cells were subjected to ultrasonication (72 cycles, 4 s each) to rupture them. The resultant mixture was subjected to centrifugation at 15,000 × g for 30 min. This supernatant was collected and introduced onto a column packed with nickel-Sepharose™ 6 Fast Flow (manufactured by GE Healthcare). Prior to sample loading, the column was equilibrated with buffer A. Elution of the target protein PCHeplII was accomplished by using buffer A containing a linear concentration of imidazole that ranged from 0 to 500 mM, and then the 250 mM eluate was collected. The protein samples were reduced and then assessed by performing SDS-PAGE using a 12% (w/v) gel to ensure the purity and molecular weight of purified PCHeplII. ImageJ software was applied to calculate the purity of PCHeplII. To ensure removal of impurities, overnight dialysis at 4°C was conducted. The protein concentration of the purified PCHeplII was quantified by employing a bicinchoninic acid (BCA) protein assay kit manufactured by Sangon Biotech in Shanghai, China.

Substrate specificity analysis of recombinant PCHeplII

To explore the substrate specificity of PCHeplII, a variety of polysaccharides were employed as substrates, including HA, CS, DS, HP, HS, and alginate. To completely degrade the polysaccharide substrates (1 mg/mL), 6 µg of the enzyme was introduced into 50 mM sodium phosphate buffer (NaH₂PO₄-Na₂HPO₄ buffer) (pH 8.0) and incubated at 30°C for 24 h. To establish a negative control, the same amount of inactivated enzyme was applied to the negative control group. Following the digestion reaction, the system was subjected to several procedures: boiling for 10 min to halt the reaction, cooling in an ice-water bath for 5 min, and centrifugation at 12,000 rpm for 10 min to eliminate insoluble matter. Subsequently, the acquired supernatants were analysed for unsaturated products based on solution absorbance at 232 nm or gel filtration high-performance liquid chromatography (HPLC).

Biochemical characterization investigation of PCHeplII

The impact of temperature on PCHeplII enzyme activity was investigated by establishing reaction systems with HP as a substrate in 50 mM sodium phosphate buffer (pH 8.0) at temperatures ranging from 0 to 70°C for a duration of 30 min. To determine the optimal reaction buffer and pH, various reaction buffers, including NaAc-HAc buffer (50 mM, pH 5.0–6.0), sodium phosphate buffer (50 mM, pH 6.0–8.0), and Tris-HCl buffer (50 mM, pH 7.0–10.0), were employed. To determine the thermostability of PCHeplII, the enzyme was incubated at varying temperatures (0–50°C) for 0 h to 24 h, and residual enzyme activity on HP was measured at the optimal temperature and pH. The effects of metal ions, chelators and LiCl on the HP-degrading activity of PCHeplII were determined via supplementation with various metal ions/chelators at a concentration of 5 mM and different concentrations of LiCl or NaCl ranging from 0–500 mM. The metal ions and chelators included Li⁺, K⁺, Na⁺, Ag⁺, Ca²⁺, Mg²⁺, Mn²⁺, Ni²⁺, Co²⁺, Hg²⁺, Cd²⁺, Zn²⁺, Pb²⁺, Fe²⁺, Ba²⁺, Cu²⁺, Fe³⁺, Cr³⁺, EDTA, imidazole, glycerol, SDS, β-mercaptoethanol and DTT. All assays were carried out in triplicate. The PCHeplII activity value was determined by averaging the absorbance at 232 nm for parallel reaction solutions.

To obtain the enzyme activity of PCHeplII on HP and HS, reaction systems containing 30 µL of enzyme (1 µg/µL), 30 µL of HP or HS (10 mg/mL), 10 µL of LiCl (3 M), 10 µL of BaCl₂ (150 mM), 100 µL of sodium phosphate buffer (150 mM, pH 7.0) and 150 µL of deionized water were employed. Incubation of the samples was carried out at 20°C for 0–5 min, after which boiling water was applied for 10 min to halt the digestion reaction. Determination of PCHeplII activity involved measuring the absorbance change per min at 232 nm, with an extinction coefficient of 3800 M⁻¹ cm⁻¹ for degradation products [1 U = 1 µmol of unsaturated carbon bond-containing product formed per min].

To test the kinetic parameters (K_m and V_{max}) of PCHeplII, the enzyme activities using different concentration of HP at the optimal reaction condition were measured. Kinetic parameters were derived from Michaelis-Menten representations.

Anion exchange HPLC analysis of the reaction system with PCHeplII and PHHeplII

Anion exchange HPLC was applied to analyse the final products of HP and HS degradation by PCHeplII. Each 30 µg of HP and HS was treated with 1.2 mU PCHeplII or PHHeplII at 20°C or 37°C for 24 h. The reaction mixtures were boiled for 10 min and centrifuged at 15,000 × g for 10 min. Then, the samples were filtered through 0.22 µm filters followed by analysis using anion exchange HPLC on a Pack Polyamine II column (YMC). The elution process was performed using a linear NaH₂PO₄ gradient of 0.016–1.0 M at a flow rate of 1.0 mL/min over a 60 min period, and the fractions were monitored at 232 nm using a UV detector. Standard unsaturated disaccharides were coinjected, and their retention times were compared to identify reaction products.

Polysaccharide degradation mode analysis of PCHeplII

To investigate the PCHeplII degradation mode of polysaccharides, a reaction system containing 100 μL of enzyme (0.2 $\mu\text{g}/\mu\text{L}$), 100 μL of HP (10 mg/mL), 100 μL of LiCl (1 M), 33 μL of BaCl_2 (150 mM), 333 μL of sodium phosphate buffer (150 mM, pH 7.0) and 334 μL of deionized water was employed. The mixture was then incubated at 20°C for 0 min, 10 min, 30 min, 1 h, 2 h, and 24 h. During this incubation period, 60 μL samples of the reaction mixture were extracted and boiled for 10 min. The samples were centrifuged at 15,000 $\times g$ for 10 min and then filtered through 0.22 μm filters followed by analysis using gel filtration HPLC on a Superdex 30 Increase 10/300 GL column (Cytiva). The elution process was performed using 0.2 M NH_4HCO_3 at a flow rate of 0.4 mL/min, and the fractions were monitored at 232 nm using a UV detector.

Effects of fluorescence labelling on the digestion of oligosaccharides by PCHeplII

To examine the influence of fluorescence labelling on the degradation of oligosaccharides by PCHeplII, unsaturated HP oligosaccharides tetrasaccharide (UDP4) and hexasaccharide (UDP6) were subjected to 2-AB labelling³³. Next, 0.5 μg of the labelled samples were treated with 1 mU of PCHeplII under the optimal conditions. The samples were subjected to a 10 min boiling procedure and were subsequently filtered using 0.22 μm filters. The resulting supernatants were assessed with gel filtration HPLC (Thermo Fisher UltiMate 3000) on a Superdex 30 Increase 10/300 GL column (Cytiva). The elution was carried out with 0.2 M NH_4HCO_3 at a flow rate of 0.4 mL/min. To monitor the process, a fluorescence detector with excitation and emission wavelengths of 330 and 420 nm, respectively, was utilized.

Substrate size preference analysis of PCHeplII

To investigate the substrate size preference of PCHeplII, a variety of unsaturated HP oligosaccharides with different size types were applied. Specifically, 2 nmol of each of the unsaturated HP oligosaccharides (UDP4, UDP6, UDP8, and UDP10) was treated with 0.16 μU PCHeplII at the optimal conditions for various time intervals: 0 min, 1 min, 5 min, 10 min, and 30 min. The samples were extracted from the reaction system, boiled for 10 min and then filtered using 0.22 μm filters. Subsequently, the samples were analysed via UV gel-filtration HPLC as described in Sect. “Polysaccharide degradation mode analysis of PCHeplII”.

Site-directed mutagenesis of PCHeplII

To determine the active centre of PCHeplII, the 3D structure of PCHeplII was modelled using Swiss Model online software (<https://swissmodel.expasy.org/>), with the Hepase II structure (PDB code: 2FUT) as the template. The candidate residues His¹⁹⁹, Tyr²⁵⁴, and His⁴⁰³ were selected for further analysis according to alignment with the active sites of PHHepII and mutated to Ala using the Mut Express II Fast Mutagenesis Kit V2 (Vazyme, Nanjing, China). The primers included H199A-F: TAGCATTACGAGCGCGACGAGCGAATGGATGCTGAT, H199A-R: TCGCGCTCGTAATGCTATACTGTTAATCGGC, Y254A-F: AACAGCGGTACAACGTGCGC TTTAGCAGCGA, Y254A-R: ACGTTGTACGCGCTGTTGCCTTGATGATAGGTATG, and H403A-F: TTCTGA ACGCGCAGCATCATGACGCGGGCGCG. The residual enzyme activities of the mutants PCHeplII-H199A, PCHeplII-Y254A, and PCHeplII-H403A towards HP and HS were analysed as described in 2.4 and 2.5.

Results

Sequence features of the PCHeplII gene and protein

The length of the gene that encodes PCHeplII is 2310 bp, and its GC content is 40.78%. PCHeplII is a protein that consists of 769 amino acids. At the N-terminus, it contains a signal peptide consisting of 23 amino acids. The molecular mass of the PCHeplII protein was calculated to be 88.26 kDa, and it has an isoelectric point value (pI) of 7.00. Analysis of the sequence revealed that PCHeplII possesses three conserved domains. These domains include a DUF4962 superfamily domain at the N-terminus (Pro⁴²-Pro³¹²), a Hepar_II_III superfamily domain on the interior (His⁴⁰³-Pro³¹²), and a HepII_C domain at the C-terminus (Ile⁶⁸⁴-Arg⁷⁶⁹) (Fig. 2A). Phylogenetic analysis showed that PCHeplII was closely related to other identified Hepases II (Fig. 2B), particularly the Hepase II (PHHepII) from *P. heparinus* DSM 2366, a commercial Hepase II. Further similarity analysis revealed that PCHeplII shares the highest amino acid identity of 68.07% with PHHepII (GenBank code: AAB18277.1)¹⁴. These results suggested that PCHeplII can be inferred to be a novel Hepase and may function similarly to Hepase II, which degrades HP and HS.

Heterologous expression and purification of recombinant PCHeplII

The recombinant plasmid pET30a-*pcheplII* was synthesized by GENEWIZ, Inc. (Suzhou, China) and successfully overexpressed the soluble protein without the signal peptide in *E. coli* BL21 (DE3) at 16°C. As shown in Fig. 3, the intracellular target protein PCHeplII was released into the supernatant after the cells were subjected to ultrasonication and centrifugation. The soluble fractions were then purified using a Ni²⁺ affinity column based on the (His)₆-tag. The SDS-PAGE results indicated that the purification procedure was highly effective, resulting in a single band, and the purity of purified PCHeplII was calculated to be 100%. Based on a comparison with the prestained protein marker, the molecular weight of the single band was estimated to be approximately 90 kDa, which is consistent with the theoretical molecular weight (88.26 kDa) of PCHeplII.

Biochemical characterization of recombinant PCHeplII

Substrate specificity experiments demonstrated that PCHeplII displayed a notable variation in the degradation of different substrates. Specifically, PCHeplII effectively degraded HP (Supplementary Fig. 1A), exhibited weak degradation of HS (Supplementary Fig. 1B), and showed no activity towards substrates such as HA, CS, DS,

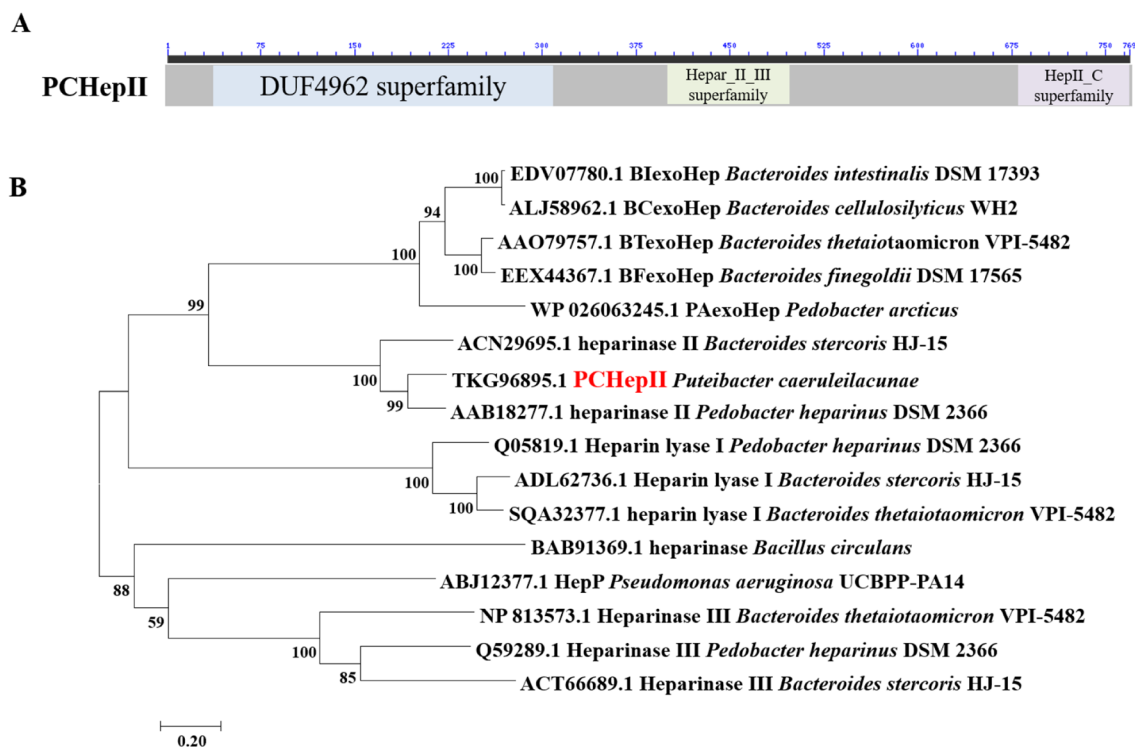


Figure 2. Module organization (A) and phylogenetic analysis (B) of PCHEP II. MEGA was used to conduct a phylogenetic analysis with the neighbour-joining method, resulting in taxa clustering together during the 1000 bootstrap test.

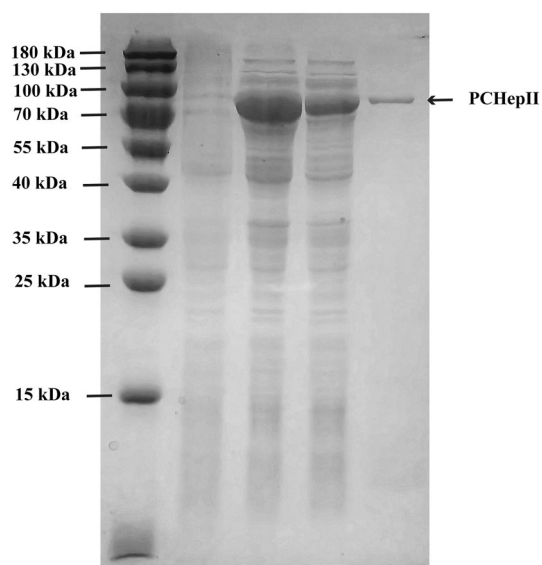


Figure 3. SDS-PAGE analysis of recombinant PCHEP II expressed in *E. coli*. Coomassie brilliant blue was used to stain 12% (w/v) SDS-PAGE gels for the analysis of the crude extract and purified PCHEP II. Lane 1, pre-stained protein standard marker (15–180 kDa); Lane 2, uninduced cell lysate of *E. coli*-pET30a; Lane 3, IPTG-induced cell lysate of *E. coli*-pET30a-*pchepII*; Lane 4, the induced lysate supernatant of *E. coli*-pET30a-*pchepII*; Lane 5, purified PCHEP II after Ni²⁺ affinity chromatography.

and alginate (Supplementary Fig. 1C–F). These findings indicate that the recombinant PCHEP II functioned as a Heparase that primarily catalyses the high-sulfated substrate HP, rather than the low-sulfated substrate HS.

Biochemical characterization experiments were conducted to optimize the enzyme activity of PCHEP II. The impact of temperature on PCHEP II enzyme activity was tested over a temperature range of 0°C to 70°C. The maximum activity based on the production of unsaturated degradation products was observed at 20°C, and the

activity sharply declined when the temperature was over 30°C (Fig. 4A). To assess the thermostability of PCHEP II, its enzyme activity was examined under various temperature conditions ranging from 0°C to 50°C. The results showed that PCHEP II was relatively stable at 0–30°C (Fig. 4E). The stability of PCHEP II sharply declined when the temperature was higher than 30°C. To test the influence of different reaction buffers and pH values on the HP-degrading activity of PCHEP II, NaAc-HAc buffer (50 mM, pH 5.0–6.0), sodium phosphate buffer (50 mM, pH 6.0–8.0), and Tris-HCl buffer (50 mM, pH 7.0–10.0) were employed. The results revealed that the highest HP-degrading activity occurred at pH 7.0 in the sodium phosphate buffer (Fig. 4B), and other pH values may have a negative impact on the enzyme activity of PCHEP II.

Moreover, the impact of various chemicals and metal ions (5 mM), including Li⁺, K⁺, Na⁺, Ag⁺, Ca²⁺, Mg²⁺, Mn²⁺, Ni²⁺, Co²⁺, Hg²⁺, Cd²⁺, Zn²⁺, Pb²⁺, Fe²⁺, Ba²⁺, Cu²⁺, Fe³⁺, Cr³⁺, EDTA, imidazole, glycerol, SDS, β-mercaptoethanol and DTT, on the enzyme activity of PCHEP II was investigated under optimum conditions (Fig. 4C). The presence of specific divalent cations, including Mg²⁺, Mn²⁺, and Ba²⁺, substantially enhanced the

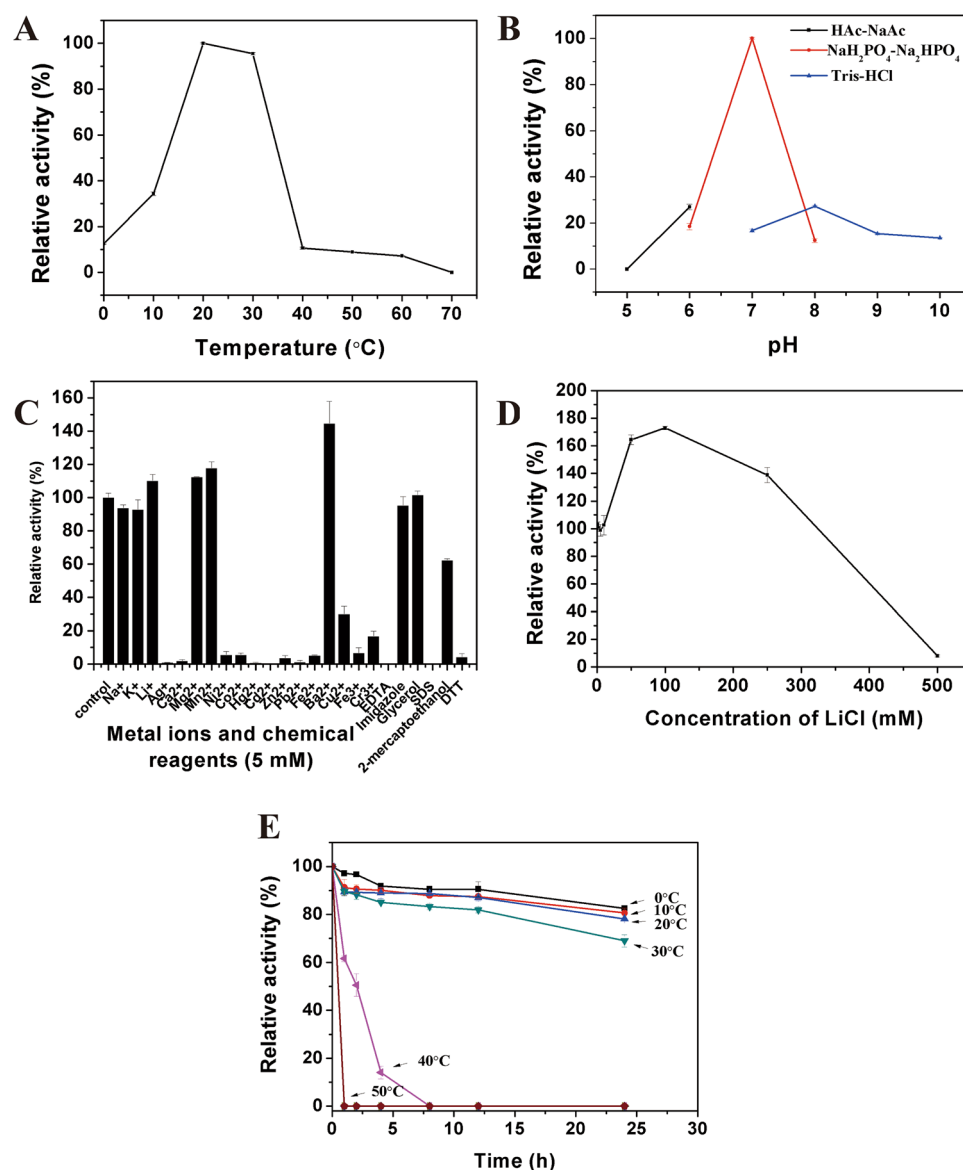


Figure 4. Biochemical characterization of recombinant PCHEP II. (A) Effect of temperature on PCHEP II activity. The highest activity observed at 20°C on HP was set at 100%. (B) Effect of pH on PCHEP II activity. The highest activity observed in the 50 mM sodium phosphate buffer (pH 7.0) on HP was set as 100%. (C) Effect of metal ions and chelators including Li⁺, K⁺, Na⁺, Ag⁺, Ca²⁺, Mg²⁺, Mn²⁺, Ni²⁺, Co²⁺, Hg²⁺, Cd²⁺, Zn²⁺, Pb²⁺, Fe²⁺, Ba²⁺, Cu²⁺, Fe³⁺, Cr³⁺, EDTA, imidazole, glycerol, SDS, β-mercaptoethanol and DTT on PCHEP II activity. The enzyme activity on HP obtained without the inclusion of tested metal ions and chemicals was considered as 100%. (D) Effect of KCl concentration on PCHEP II activity. The activity of PCHEP II without LiCl was set as 100%. (E) Thermostability of PCHEP II. The residual activity of PCHEP II on HP without preincubation was set at 100%.

HP-degrading activity of PCHEP2. Among these cations, Ba^{2+} exhibited the most pronounced positive effect, resulting in a 145% increase in activity (Fig. 4C). Conversely, the addition of EDTA completely inhibited the enzyme activity of PCHEP2, implying the essential role of divalent cations in its catalytic function. On the other hand, chemicals and metal ions, including Na^+ , K^+ , imidazole, and glycerol, did not show an obvious influence on PCHEP2 enzyme activity; β -mercaptoethanol slightly inhibited PCHEP2 enzyme activity; Ni^{2+} , Co^{2+} , Zn^{2+} , Cu^{2+} , Fe^{2+} , Fe^{3+} , Cr^{3+} , and DTT severely inhibited the HP-degrading activity of PCHEP2; and Ca^{2+} , Ag^+ , Pb^{2+} , Hg^{2+} , Cd^{2+} , and SDS completely inhibited the HP-degrading activity of PCHEP2. Additionally, the presence of LiCl greatly stimulated the HP-degrading activity of PCHEP2, with the most significant enhancement (173%) observed at a concentration of 100 mM (Fig. 4D). Even at a concentration of 250 mM, enzyme activity was enhanced (Fig. 4D). However, the presence of NaCl in the reaction system did not significantly stimulate the activity of PCHEP2, the use of 100 mM NaCl resulted in a 113% increase in enzyme activity (Supplementary Fig. 2).

The specific activity and kinetic parameters of PCHEP2 towards HP were measured by calculating the absorbance change per min at 232 nm. As a result, the enzyme activity of PCHEP2 towards HP was measured to be 254 mU/mg protein, and the V_{max} and K_m of PCHEP2 were calculated as 494 mU/mg protein and 0.33 mg/mL, respectively. While, the enzyme activity towards HS was too low to measure, although PCHEP2 could partially degrade HS (Supplementary Fig. 1B). These results suggest that the novel PCHEP2 exhibits a stronger preference for catalysing high-sulfated HP rather than low-sulfated HS.

Anion exchange HPLC analysis of the reaction system with PCHEP2 and PHHEP2

The final products of HP and HS degradation by PCHEP2 and PHHEP2 were analysed via anion exchange HPLC. The results showed that the final products of HP degradation by PCHEP2 and PHHEP2 were similar and were mainly composed of the trisulfated disaccharide $\Delta\text{UA}2\text{S}1\text{-}4\text{GlcNS}6\text{S}$ and a small quantity of the disulfated disaccharides $\Delta\text{UA}2\text{S}1\text{-}4\text{GlcNS}$ and $\Delta\text{UA}1\text{-}4\text{GlcNS}6\text{S}$ (Fig. 5A). The final products of HS degradation by PCHEP2 were composed of the trisulfated disaccharide $\Delta\text{UA}2\text{S}1\text{-}4\text{GlcNS}6\text{S}$ and the disulfated disaccharides $\Delta\text{UA}2\text{S}1\text{-}4\text{GlcNS}$ and $\Delta\text{UA}1\text{-}4\text{GlcNS}6\text{S}$ (Fig. 5B). The final products of HS degradation by PHHEP2 were composed of the trisulfated disaccharide $\Delta\text{UA}2\text{S}1\text{-}4\text{GlcNS}6\text{S}$, the disulfated disaccharides $\Delta\text{UA}2\text{S}1\text{-}4\text{GlcNS}$ and $\Delta\text{UA}1\text{-}4\text{GlcNS}6\text{S}$, the monosulfated disaccharides $\Delta\text{UA}1\text{-}4\text{GlcNS}$ and $\Delta\text{UA}1\text{-}4\text{GlcNAc}6\text{S}$, and the nonsulfated disaccharide $\Delta\text{UA}1\text{-}4\text{GlcNAc}$ (Fig. 5B). The results indicated that PCHEP2 preferred to degrade the high-sulfated regions of HP and HS, while PHHEP2 could degrade both the high-sulfated and low-sulfated regions of HP and HS.

Polysaccharide degradation mode of PCHEP2

The mechanism of PCHEP2 action was studied via the degradation of HP under optimal conditions for 0–24 h. Reaction solutions for quantification were collected at regular time intervals and analysed using HPLC at 232 nm. Initially, the primary degradation (30 min as an example) products of PCHEP2 were unsaturated oligosaccharides with high molecular weights, as shown in Supplementary Fig. 3. As the reaction time increased, the molecular size of these unsaturated oligosaccharides gradually decreased, eventually forming unsaturated disaccharides. These findings indicate that PCHEP2 is an endo-type Heparase, as shown in Fig. 6.

Influence of fluorescence labelling on PCHEP2

Fluorescence labelling is commonly used in the structural analysis of GAGs³⁴. However, it has been observed that the fluorophores located at the end of the GAG chains often affect the degradation processes carried out by

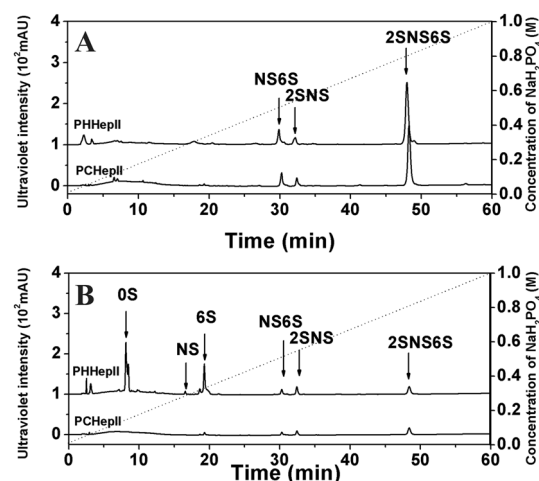


Figure 5. Final products of HP and HS degraded by PCHEP2 and PHHEP2. The final products of HP (A) and HS (B) by PCHEP2 and PHHEP2 were analyzed via the anion exchange HPLC. OS, $\Delta\text{UA}(1\text{--}4)\text{GlcNAc}$; 6S, $\Delta\text{UA}(1\text{--}4)\text{GlcNAc}6\text{S}$; 2S, $\Delta\text{UA}2\text{S}(1\text{--}4)\text{GlcNAc}$; NS, $\Delta\text{UA}(1\text{--}4)\text{GlcNS}$; 2S6S, $\Delta\text{UA}2\text{S}(1\text{--}4)\text{GlcNAc}6\text{S}$; NS6S, $\Delta\text{UA}(1\text{--}4)\text{GlcNS}6\text{S}$; 2SNS, $\Delta\text{UA}2\text{S}(1\text{--}4)\text{GlcNS}$; 2SNS6S, $\Delta\text{UA}2\text{S}(1\text{--}4)\text{GlcNS}6\text{S}$.

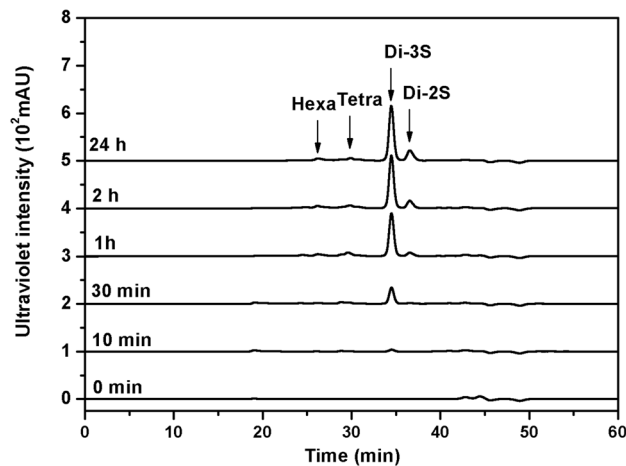


Figure 6. Polysaccharide degradation pattern analysis of recombinant PCHEP II with HP as substrate. Purified PCHEP II was used to treat HP (1 mg/mL) at 20°C in 50 mM sodium phosphate buffer (pH 7.0) for 0–24 h. Samples of 30 µg were taken at intervals for gel filtration HPLC analysis. The degree of depolymerization of HP unsaturated oligosaccharides released from the polysaccharide substrates by the digestion of HP are indicated by arrows: Hexa, HP unsaturated hexasaccharide; Tetra, HP unsaturated tetrasaccharide; Di-3S, the trisulfated HP unsaturated disaccharides; Di-2S, the disulfated HP unsaturated disaccharides.

lyases³⁵. To investigate the impact of fluorescence labelling on the digestion capacity of PCHEP II, the HP oligosaccharides UDP4 and UDP6 were labelled with 2-AB (2-aminobenzamide) and then treated with PCHEP II. The results showed that PCHEP II could digest 2-AB-UDP6 to form 2-AB-UDP4 (Fig. 7B), but it was unable to generate 2-AB-UDP2 from 2-AB-UDP4 (Fig. 7A). While, PCHEP II could efficiently degrade the unlabeled UDP4 (Supplementary Fig. 4A) and UDP6 (Supplementary Fig. 4B) to generate the disaccharide products. These findings suggested that PCHEP II could not degrade the 2-AB-labelled tetrasaccharides, possibly because the fluorophores at the reducing end hampered the interaction of 2-AB-UDP4 with the active centre of PCHEP II.

Substrate size preference of PCHEP II

To determine the substrate preference of PCHEP II, unsaturated HP oligosaccharides of various sizes (UDP4, UDP6, UDP8, and UDP10) were employed and treated with PCHEP II for time intervals ranging from 0 to 30 min. Figure 8A and B show changes in the unsaturated products and the monitored substrates, respectively. As time progressed, the amounts of unsaturated products increased and exhibited different trends (Fig. 8A). The production rate of unsaturated products formed from the degradation of UDP4 by PCHEP II is higher than that of other oligosaccharides, especially at 5 min (Fig. 8A). Additionally, Fig. 8B demonstrates that the degradation rate of UDP4 was significantly higher than that of other oligosaccharides throughout the reaction process. These findings suggested that PCHEP II prefers to catalyse smaller substrates, which explains why PCHEP II generates small amounts of larger oligosaccharides when digesting HP polysaccharides in the early degradation stage (Fig. 6). This is because PCHEP II primarily catalyses small-sized substrates after disrupting the polysaccharides, resulting in relatively lower enzyme activity towards HP polysaccharides.

Mutagenesis study of PCHEP II

To investigate the catalytic mechanism of the enzyme, the simulated structure of PCHEP II was established using Swiss Model online software. Candidate active sites, including His¹⁹⁹, Tyr²⁵⁴, and His⁴⁰³ (Fig. 9A), consistent with the active sites His²⁰², Tyr²⁵⁷, and His⁴⁰⁶ of PHHEP II¹⁵, were selected and then mutated to Ala individually. The mutants PCHEP II-H199A and PCHEP II-H403A completely lost enzyme activity towards the HP substrate (Fig. 9B), and the mutant PCHEP II-Y254A retained the ability to catalyse HP (Fig. 9B), while the exact enzyme activity of PCHEP II-Y254A was too low to be exactly calculated. These results indicated that the His¹⁹⁹, Tyr²⁵⁴, and His⁴⁰³ residues play crucial roles in the catalytic action of PCHEP II and may serve as the active centre.

Discussion

Hepases are a large class of polysaccharide lyases that play a crucial role in HP and HS structural studies and in the preparation of LMWHs¹. In recent decades, several hepases have been reported and can be classified into three categories: hepase I, hepase II, and hepase III²⁹. However, these identified hepases were all derived from terrestrial bacteria, and hepases derived from marine bacteria are still unknown³⁰. Due to significant differences in environment, hepases derived from marine bacteria may exhibit unique characteristics and have the potential to generate new products when applied in the production of HP oligosaccharides. In this study, a novel hepase named PCHEP II, which was derived from the marine bacterium *Puteibacter caeruleilacunae*, was studied in detail.

Phylogenetic analysis revealed that PCHEP II clusters with the Hepase II clades and shares the highest similarity of 68.07% with PHHEP II¹⁵. Therefore, PCHEP II can be considered a new member of the Hepase II family.

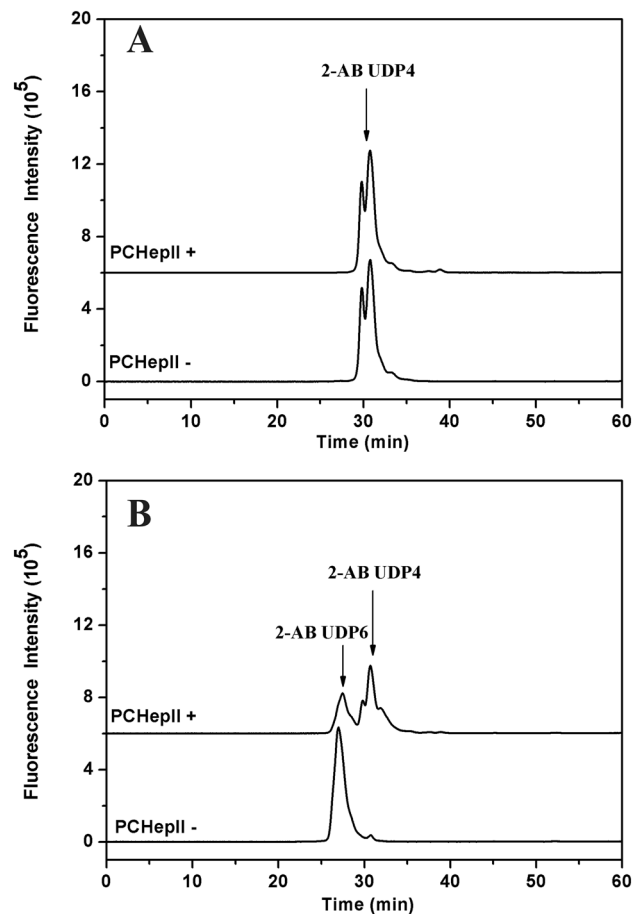


Figure 7. 2-AB labeled oligosaccharides digestion analysis of PCHeplI. 2 μ g of the HP UDP4 (A) and UDP6 (B) were 2-AB labeled and then treated with excessive PCHeplI for overnight. The samples were filtered and analyzed gel filtration HPLC with a fluorescence detector.

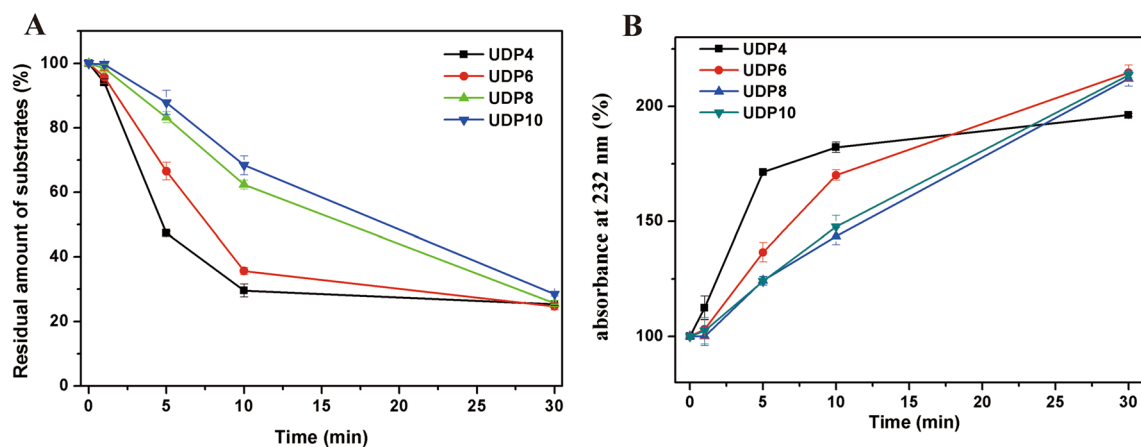


Figure 8. Size defined substrates degradation analysis by PCHeplI. Each 2 nmol of the size defined substrates including UDP4, UDP6, UDP8 and UDP10 were treated with PCHeplI for 0 min, 1 min, 5 min, 10 min, and 30 min. And then the samples were analyzed by UV gel-filtration HPLC and calculate the production of the unsaturated products (A) and residual amount of the substrates (B). Each data was shown as the mean of three replicates \pm standard deviation.

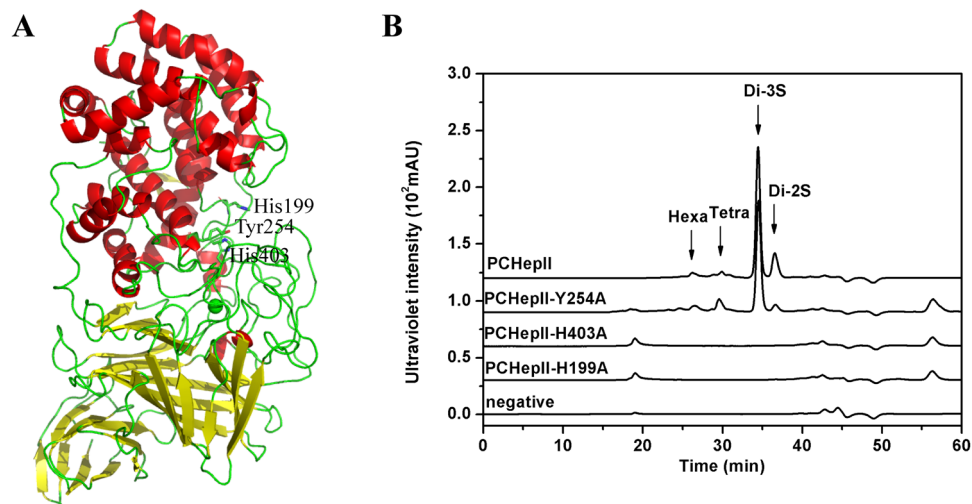


Figure 9. Simulated structure (A) and mutagenesis analysis (B) of PCHEP II. (A) The structure of PCHEP II was simulated via the Swiss Model online software. (B) The mutants PCHEP II-H199A, PCHEP II-Y254A, and PCHEP II-H403A were applied to treat HP for overnight and then analyzed by the gel filtration HPLC. Hexa, HP unsaturated hexasaccharide; Tetra, HP unsaturated tetrasaccharide; Di-3S, the trisulfated HP unsaturated disaccharides; Di-2S, the disulfated HP unsaturated disaccharides.

However, it was surprising that PCHEP II showed a preference for catalysing HP substrates rather than HS substrates, as it did not effectively degrade HS. Furthermore, analysis of the final HP and HS degradation products with PCHEP II showed that the enzyme mainly generates highly sulfated disaccharides, including the trisulfated disaccharide Δ UA2S1-4GlcNS6S and the disulfated disaccharides Δ UA2S1-4GlcNS and Δ UA1-4GlcNS6S. While the final products of HP and HS, especially HS, consist of trisulfated and disulfated disaccharides, a large amount of the monosulfated disaccharides Δ UA1-4GlcNS and Δ UA1-4GlcNAc6S and the nonsulfated disaccharide Δ UA1-4GlcNAc were also observed. These characteristics clearly showed that PCHEP II preferred to catalyse the highly sulfated regions of HP and HS, and the characteristics were different from those of the identified heparinase II enzymes, which do not exhibit such substrate selectivity between HP and HS substrates^{36,37}. Instead, the preference of PCHEP II for degrading highly sulfated HP polysaccharides aligns more closely with heparinase I^{36,37}. This suggested that PCHEP II could be classified as a novel type of Heparinase, despite its high similarity to the heparinase II family.

PCHEP II showed higher activity at neutral pH and temperatures of 20°C and 30°C, similar to other GAG lyases found in marine bacteria³⁰, consistent with marine environmental conditions. The optimal temperature for PCHEP II was completely different from that of PHHEP II (optimal temperature of 40°C) and other identified Heparinase II²¹. PCHEP II remained stable at 0–30°C even after 24 h and retained 78% of its enzyme activity. However, its stability drastically decreased at temperatures above 40°C, suggesting that PCHEP II is a hypothermophilous enzyme. Additionally, PCHEP II was more activated in a high salt environment, and the enzyme activity of PCHEP II was enhanced with 100 mM KCl or NaCl. Even when the concentration of KCl or NaCl reached 250 mM, the enzyme activity of PCHEP II was enhanced (KCl) or was not significantly affected (NaCl). This phenomenon was not observed in PHHEP II, which was inhibited by salt²¹. These characteristics indicated that the marine-derived heparinase PCHEP II was different from terrestrial heparinases and was more adapted to a marine environment.

The activity of PCHEP II was significantly enhanced by the presence of 5 mM Ba^{2+} (145%), while it was completely inhibited by EDTA, indicating the essential role of divalent cations in its activity. However, for PHHEP II, none of the divalent cations could enhance the activity of PHHEP II²¹. Other heavy metal ions, including Ni^{2+} , Co^{2+} , Zn^{2+} , Cu^{2+} , Fe^{2+} , Fe^{3+} , Cr^{3+} , Ca^{2+} , Ag^{+} , Pb^{2+} , Hg^{2+} , and Cd^{2+} , could inhibit the enzyme activity of PCHEP II, similar to PHHEP II²¹. These results indicate that heavy metal ions may have impeded the reaction of heparinases with substrates. The enzyme activity of PCHEP II towards HP was calculated to be 254 mU/mg protein, and the exact enzyme activity towards HS was too low to be measured, although PCHEP II could slowly degrade HS. The enzyme activities of PCHEP II towards the substrates were far less than those of PHHEP II, for which the enzyme activities towards HP and HS were 19 U/mg protein and 36.5 U/mg protein³⁸, respectively. The results indicated that the enzyme activity of marine-derived heparinases may be lower than that of terrestrial heparinases, and this difference should be further analysed via the identification of more marine-derived heparinases.

Similar to Heparinase II, PCHEP II exhibited an endolyase form when degrading substrates¹. However, it is interesting to note that PCHEP II primarily generates disaccharide products during the catalytic stages, with a relatively low amount of larger oligosaccharides. Typically, endolyases randomly digest polysaccharide chains, resulting in a higher production of larger oligosaccharides in the early stages of digestion, which are then converted to disaccharides³⁹. Further testing revealed that PCHEP II showed a preference for catalysing small-sized substrates, particularly HP tetrasaccharides. The results indicated that when PCHEP II degrades substrates, it may randomly combine with the chains and then combine with the generated unsaturated oligosaccharides and sequentially

catalyse the release of disaccharides from the oligosaccharides, which explains why disaccharide peaks dominate the products throughout the digestion stages. Consequently, the enzyme activity of PCHeP2 towards HP is relatively low.

Fluorescence labelling is a common and straightforward method used in structural studies of GAGs³⁴. Lyases that can breakdown 2-AB labelled disaccharides from oligosaccharides are valuable tools and have already been utilized in the structural studies of chondroitin sulfate³⁵. However, for HP/HS, studies of this type of enzyme were relatively scarce. PCHeP2 was able to breakdown 2-AB-labelled hexasaccharides and generated 2-AB-labelled tetrasaccharides, but it was inactive towards 2-AB-labelled tetrasaccharides. This indicated that the fluorophore 2-AB at the reducing end of the oligosaccharides may impede necessary interactions between the substrates and the active centre of PCHeP2 and thus reduce the degradation capacity of PCHeP2.

The His¹⁹⁹, Tyr²⁵⁴, and His⁴⁰³ residues were selected as candidate active centre residues through alignment with PHHeP2⁴⁰. The mutants PCHeP2-H199A, PCHeP2-Y254A, and PCHeP2-H403A were tested for residual enzyme activity using HP polysaccharides as substrates. The enzyme activities of the mutants were either completely absent or greatly reduced. Therefore, it can be concluded that the three residues His¹⁹⁹, Tyr²⁵⁴, and His⁴⁰³ form the active centres of PCHeP2 and are essential for stabilizing and facilitating proton transfer in HP/HS substrates.

Conclusions

In this study, a marine bacteria-derived heparinase, PCHeP2, was studied in detail, and its characteristics were examined. PCHeP2 demonstrated excellent solubility and expression levels, making it suitable for industrial production. Additionally, PCHeP2 exhibited preferential activity in environments with intermediate to low temperatures and high salt concentrations, which are conditions commonly found in marine environments. Despite having endo-lyase activity, PCHeP2 displayed higher activity towards small substrates. This is the first study to report the marine-derived heparinase, PCHeP2, and the results might provide a potential approach for HP and HS research in the future.

Data availability

All data generated or analysed during this study are included in this published article. The original gel figure of PCHeP2 was shown in supplementary data.

Received: 21 August 2023; Accepted: 14 November 2023

Published online: 17 November 2023

References

- Casu, B., Naggi, A. & Torri, G. Re-visiting the structure of heparin. *Carbohydr. Res.* **403**, 60–68 (2015).
- Tsai, C. T., Zulueta, M. M. L. & Hung, S. C. Synthetic heparin and heparan sulfate: Probes in defining biological functions. *Curr. Opin. Chem. Biol.* **40**, 152–159 (2017).
- Lindahl, U., Kusche-Gullberg, M. & Kjell n, L. Regulated diversity of heparan sulfate. *J. Biol. Chem.* **273**, 24979–24982 (1998).
- Sasisekharan, R. & Venkataraman, G. Heparin and heparan sulfate: Biosynthesis, structure and function. *Curr. Opin. Chem. Biol.* **4**, 626–631 (2000).
- Capila, I. & Linhardt, R. J. Heparin-protein interactions. *Angew. Chem. Int. Ed. Engl.* **41**, 391–412 (2002).
- Hogwood, J., Mulloy, B., Lever, R., Gray, E. & Page, C. P. Pharmacology of heparin and related drugs: An update. *Pharmacol. Rev.* **75**, 328–379 (2023).
- Hayashida, K., Aquino, R. S. & Park, P. W. Coreceptor functions of cell surface heparan sulfate proteoglycans. *Am. J. Physiol. Cell Physiol.* **322**, C896–C912 (2022).
- Collins, L. E. & Troeberg, L. Heparan sulfate as a regulator of inflammation and immunity. *J. Leukoc. Biol.* **105**, 81–92 (2019).
- Mang, D., Roy, S. R., Zhang, Q., Hu, X. & Zhang, Y. Heparan sulfate-instructed self-assembly selectively inhibits cancer cell migration. *ACS Appl. Mater. Interfaces* **13**, 17236–17242 (2021).
- Chen, Z. *et al.* Heparan sulfate regulates IL-21 bioavailability and signal strength that control germinal center B cell selection and differentiation. *Sci. Immunol.* **8**, eadd1728 (2023).
- Tan, C. W. *et al.* Pteropine orthoreoviruses use cell surface heparan sulphate as an attachment receptor. *Emerg. Microbes Infect.* **12**, 2208683 (2023).
- Capila, I. & Linhardt, R. J. Heparin-protein interactions. *Angew. Chem. Int. Ed. Engl.* **41**, 391–412 (2002).
- Meneghetti, M. C. *et al.* Heparan sulfate and heparin interactions with proteins. *J. R. Soc. Interface* **12**, 0589 (2015).
- Ulaganathan, T. *et al.* Conformational flexibility of PL12 family heparinases: Structure and substrate specificity of heparinase III from *Bacteroides thetaiotaomicron* (BT4657). *Glycobiology* **27**, 176–187 (2017).
- Fernandes, C. L., Escouto, G. B. & Verli, H. Structural glycochemistry of heparinase II from *Pedobacter heparinus*. *J. Biomol. Struct. Dyn.* **32**, 1092–1102 (2014).
- Hashimoto, W., Maruyama, Y., Nakamichi, Y., Mikami, B. & Murata, K. Crystal structure of *Pedobacter heparinus* heparin lyase Hep III with the active site in a deep cleft. *Biochemistry* **53**, 777–786 (2014).
- Zhang, C. *et al.* Structure-based engineering of heparinase I with improved specific activity for degrading heparin. *BMC Biotechnol.* **19**, 59 (2019).
- Hoy, S. M., Scott, L. J. & Plosker, G. L. Tinzaparin sodium: A review of its use in the prevention and treatment of deep vein thrombosis and pulmonary embolism, and in the prevention of clotting in the extracorporeal circuit during haemodialysis. *Drugs* **70**, 1319–1347 (2010).
- Kim, W. S., Kim, B. T., Kim, D. H. & Kim, Y. S. Purification and characterization of heparin lyase I from *Bacteroides stercoris* HJ-15. *J. Biochem. Mol. Biol.* **37**, 684–690 (2004).
- Hyun, Y. J., Lee, J. H. & Kim, D. H. Cloning, overexpression, and characterization of recombinant heparinase III from *Bacteroides stercoris* HJ-15. *Appl. Microbiol. Biotechnol.* **86**, 879–890 (2010).
- Hyun, Y. J., Lee, K. S. & Kim, D. H. Cloning, expression and characterization of a heparan sulfate-degrading heparin lyase II from *Bacteroides stercoris* HJ-15. *J. Appl. Microbiol.* **108**, 226–235 (2010).
- Han, Y. H. *et al.* Structural snapshots of heparin depolymerization by heparin lyase I. *J. Biol. Chem.* **284**, 34019–34027 (2009).
- Yoshida, E. *et al.* Cloning, sequencing, and expression of the gene from *Bacillus circulans* that codes for a heparinase that degrades both heparin and heparan sulfate. *Biosci. Biotechnol. Biochem.* **66**, 1873–19187 (2002).

24. Watanabe, M. *et al.* Characterization of heparinase from an oral bacterium *Prevotella heparinolytica*. *J. Biochem.* **123**, 283–288 (1998).
25. Liu, C. Y., Su, W. B., Guo, L. B. & Zhang, Y. W. Cloning, expression, and characterization of a novel heparinase I from *Bacteroides eggerthii*. *Prep. Biochem. Biotechnol.* **50**, 477–485 (2020).
26. Gao, L. W. *et al.* A highly active heparinase I from *Bacteroides cellulosilyticus*: Cloning, high level expression, and molecular characterization. *PLoS One* **15**, e0240920 (2020).
27. Li, Y. *et al.* Expression and characterization of heparinase II with MBP tag from a novel strain, *Raoultella* NX-TZ-3-15. *Arch. Microbiol.* **204**, 551 (2022).
28. Li, Y. *et al.* Cloning and expression of heparinase gene from a novel strain *Raoultella* NX-TZ-3-15. *Appl. Biochem. Biotechnol.* **194**, 4971–4984 (2022).
29. Singh, V. *et al.* Isolation, purification, and characterization of heparinase from *Streptomyces variabilis* MTCC 12266. *Sci. Rep.* **9**, 6482 (2019).
30. Zhang, Q. *et al.* Discovery of exolytic heparinases and their catalytic mechanism and potential application. *Nat. Commun.* **12**, 1263 (2021).
31. Zhang, Q., Wei, L., Guan, J., Sugahara, K. & Li, F. Marine bacteria as a rich source of Glycosaminoglycan-degrading enzymes. In *Encyclopedia of Marine Biotechnology* (ed. Kim, S.-K.) (Wiley, 2020).
32. Johnson, E. A. Heparan sulphates from porcine intestinal mucosa. Preparation and physicochemical properties. *Thromb. Res.* **35**, 583–588 (1984).
33. Zhang, Q., Lu, D. & Li, F. Enzymatic sequencing of heparin oligosaccharides using exolyase. *Methods Mol. Biol.* **2619**, 249–256 (2023).
34. Bigge, J. C. *et al.* Nonselective and efficient fluorescent labeling of glycans using 2-amino benzamide and anthranilic acid. *Anal. Biochem.* **230**, 229–238 (1995).
35. Wang, W. *et al.* Sequencing of chondroitin sulfate oligosaccharides using a novel exolyase from a marine bacterium that degrades hyaluronan and chondroitin sulfate/dermatan sulfate. *Biochem. J.* **474**, 3831–3848 (2017).
36. Desai, U. R., Wang, H. M. & Linhardt, R. J. Specificity studies on the heparin lyases from *Flavobacterium heparinum*. *Biochemistry* **32**, 8140–8145 (1993).
37. Desai, U. R., Wang, H. M. & Linhardt, R. J. Substrate specificity of the heparin lyases from *Flavobacterium heparinum*. *Arch. Biochem. Biophys.* **306**, 461–468 (1993).
38. Lohse, D. L. & Linhardt, R. J. Purification and characterization of heparin lyases from *Flavobacterium heparinum*. *J. Biol. Chem.* **267**, 24347–24355 (1992).
39. Zhang, Q. *et al.* Identification and biochemical characterization of a novel chondroitin sulfate/dermatan sulfate lyase from *Photobacterium* sp. *Int. J. Biol. Macromol.* **165**, 2314–2325 (2020).
40. Shaya, D. *et al.* Crystal structure of heparinase II from *Pedobacter heparinus* and its complex with a disaccharide product. *J. Biol. Chem.* **281**, 15525–15535 (2006).

Acknowledgements

This research was funded by the National Natural Science Foundation of China (32201039), and the Natural Science Foundation of Shandong Province (ZR2022QC247). We thank the gift of the commercial Heparase I, Heparase II and Heparase III from Fuchuan Li lab in Shandong University.

Author contributions

D.L. and Q.Z. conceived the experiments. D.L., L.W., Z.N., Z.L., M.L. and Y.J. conducted the experiments. D.L., L.W. and Z.N. analyzed the results. D.L., L.W., Z.N. and Q.Z. wrote the manuscript. All authors reviewed the manuscript.

Competing interests

The authors declare no competing interests.

Additional information

Supplementary Information The online version contains supplementary material available at <https://doi.org/10.1038/s41598-023-47493-y>.

Correspondence and requests for materials should be addressed to Q.Z.

Reprints and permissions information is available at www.nature.com/reprints.

Publisher's note Springer Nature remains neutral with regard to jurisdictional claims in published maps and institutional affiliations.



Open Access This article is licensed under a Creative Commons Attribution 4.0 International License, which permits use, sharing, adaptation, distribution and reproduction in any medium or format, as long as you give appropriate credit to the original author(s) and the source, provide a link to the Creative Commons licence, and indicate if changes were made. The images or other third party material in this article are included in the article's Creative Commons licence, unless indicated otherwise in a credit line to the material. If material is not included in the article's Creative Commons licence and your intended use is not permitted by statutory regulation or exceeds the permitted use, you will need to obtain permission directly from the copyright holder. To view a copy of this licence, visit <http://creativecommons.org/licenses/by/4.0/>.

© The Author(s) 2023